

# Direct Formation of Supermassive Black Holes via Multi-Scale Gas Inflows in Galaxy Mergers

L. Mayer<sup>1</sup>, S. Kazantzidis<sup>3</sup>, A. Escala<sup>4,5</sup>, & S. Callegari<sup>1</sup>

<sup>1</sup>Institute for Theoretical Physics, University of Zürich, Winterthurestrasse 190, 8057 Zürich, Switzerland

<sup>3</sup>Center for Cosmology and Astro-Particle Physics; and Department of Physics; and Department of Astronomy, The Ohio State University, USA

<sup>4</sup>Kavli Institute for Particle Astrophysics and Cosmology (KIPAC), Stanford University, 2575 Sand Hill Road MS 29 Menlo Park, CA, USA

<sup>5</sup>Departamento de Astronomia, Universidad de Chile, Casilla 36-D, Santiago, Chile.

---

Observations of distant bright quasars suggest that billion solar mass supermassive black holes (SMBHs) were already in place less than a billion years after the Big Bang<sup>1</sup>. Models in which light black hole seeds form by the collapse of primordial metal-free stars<sup>2,3</sup> cannot explain their rapid appearance due to inefficient gas accretion<sup>4,5,6</sup>. Alternatively, these black holes may form by direct collapse of gas at the center of protogalaxies<sup>7,8,9</sup>. However, this requires metal-free gas that does not cool efficiently and thus is not turned into stars<sup>8</sup>, in contrast with the rapid metal enrichment of protogalaxies<sup>10</sup>. Here we use a numerical simulation to show that mergers between massive protogalaxies naturally produce the required central gas accumulation with no need to suppress star formation. Merger-driven gas inflows produce an unstable, massive nuclear gas disk. Within the disk a second gas inflow accumulates more than 100 million solar masses of gas in a sub-parsec scale cloud in one hundred thousand years. The cloud undergoes gravitational collapse, which eventually leads to the formation of a massive black hole. The black hole can grow to a billion solar masses in less than a billion years by accreting gas from the surrounding disk.

---

The conventional scenario postulates that light black hole seeds form from the collapse of an early generation of metal-free (Population III) stars<sup>2,10,11</sup>. Sustained accretion of such seed black holes at or above the Eddington rate is required to grow the billion solar masses SMBHs that are thought to power bright quasars at  $z \sim 6$ <sup>3</sup>. Yet numerical simulations show that the ionized gas surrounding the seeds has very low densities and high pressures that would prevent the required high accretion rates<sup>4</sup>. Radiative feedback from accretion and radiation pressure also limit the accretion rate to values well below Eddington<sup>5,6,12</sup>.

Dynamical effects, such as the expulsion of a black hole from the host halo due to asymmetric emission of gravitational waves in mergers (the "gravitational rocket") can stifle further the growth of the seeds<sup>3,13</sup>.

Alternatively, massive black hole seeds exceeding  $10^4 M_\odot$  might form directly from runaway gas collapse at the centers of protogalaxies<sup>6,8,9,10,11,14</sup>. The accumulation of large amounts of gas in galactic nuclei can occur via efficient transport of angular momentum driven by gravitational torques in galactic disks<sup>15,16,17</sup>, via viscous diffusion due to gravito-driven turbulence<sup>18,19</sup>, or by means of the magnetorotational instability<sup>20,21</sup>. Recent models suggest that under normal thermodynamical conditions of the interstellar medium gas would be converted into stars faster than it is driven to the center<sup>16,22</sup>. Instead, large inflow rates,  $> 1 M_\odot/\text{yr}$ , could accumulate a large central gas concentration without fragmentation into stars, leading eventually to direct SMBH formation, if molecular cooling and metal cooling are suppressed<sup>8,16,22</sup>. However, even if molecular cooling can be suppressed at high redshift as  $H_2$ , the most abundant molecule, is dissociated by the cosmic ultraviolet background<sup>8,16</sup>, as soon as some metals are produced after the first generation of stars protogalaxies would still undergo rapid cooling and star formation, especially in the presence of dust<sup>10</sup>. Therefore, at present it is unclear if protogalaxies ever met the conditions required for direct SMBH formation.

Yet, current direct formation models are simple one-dimensional semi-analytical calculations that start from an initially stable, axisymmetric kiloparsec scale protogalactic gas disk, and perturb it under the assumption that the inflow occurs in a steady-state fashion<sup>8,16</sup>. Neither the initial stability and regular structure, nor the steady state condition of the inflow, are representative of galaxies at high redshift, which are subject to rapid gas accretion and repeated mergers. Moreover, due to their steady-state nature, these models cannot even demonstrate that gas inflows do really lead to a central collapse.

The solution to the rapid build-up of SMBHs may be offered by galaxy mergers. In mergers tidal torques and shock dissipation are capable of driving most of the gas content of galaxies from kiloparsec scales down to scales of several tens of parsecs at rates as high as  $10 - 100 M_\odot/\text{yr}$ , forming nuclear gas disks despite high star formation rates<sup>23,24</sup>. If such gas inflows could continue all the way down to the very center of the merger remnant at these high rates they would provide an alternative route to direct massive black hole formation<sup>10</sup>. Addressing this issue requires a three-dimensional simulation following gasdynamics across an unprecedented range of spatial scales.

We begin by performing a merger simulation between two identical disk galaxies with moderate amounts of gas<sup>23</sup>, several kiloparsecs in size and embedded in a  $10^{12} M_\odot$  halo (see Supplementary Information). In the concordance WMAP5 cosmology such objects would correspond to fairly high density peaks collapsing at  $z \sim 7 - 8^5$ , ( $\sim 4 - 5\sigma$ , where  $\sigma$  is the rms variation of the cosmological density field). Recent cosmological simulations show that massive, kiloparsec-scale rotating disks of stars and gas are already present in halos with masses  $> 10^{11} M_\odot$  at  $z > 4^{21}$ . The mass of the dark halo of each galaxy is

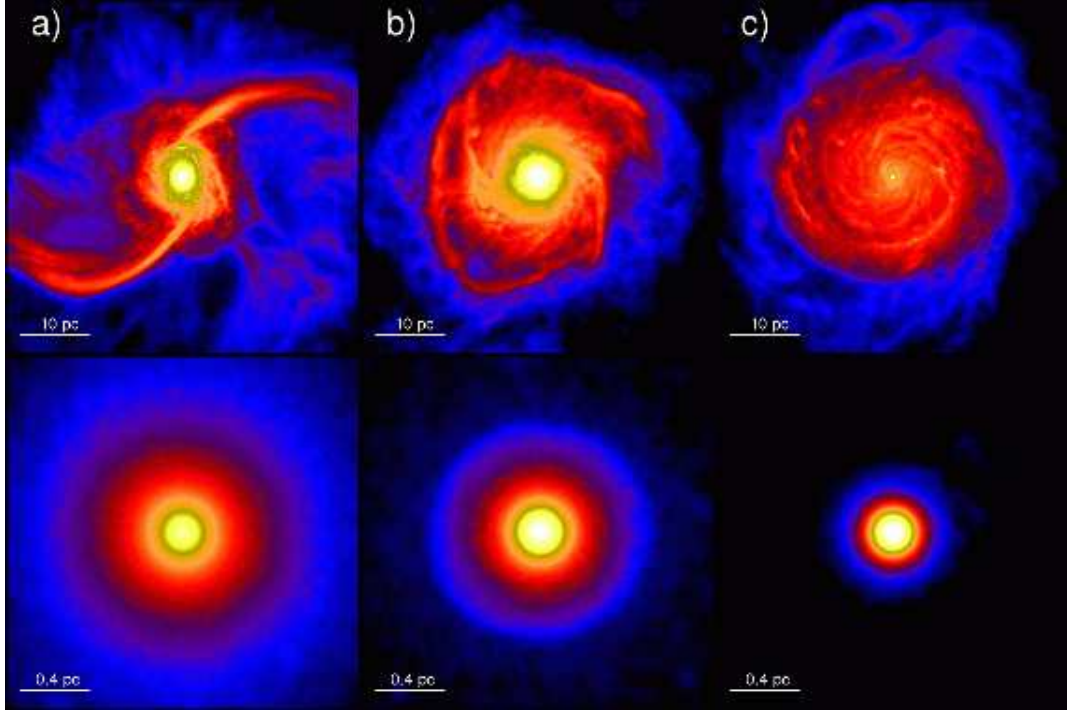


**Figure 1. Time evolution of the simulated nuclear disk.** The surface density maps of the nuclear disk are shown at both large (upper panels) and small scales (bottom panels). Particles are color-coded on a logarithmic scale with brighter colors in regions of higher density. The density ranges from  $2 \times 10^4$  to  $1 \times 10^8 M_{\odot}/pc^2$  and from  $2 \times 10^6$  to  $2 \times 10^{10} M_{\odot}/pc^2$  in the upper and lower panels, respectively. The time increases from left to right, corresponding to  $9.1 \times 10^3$  yr,  $7.49 \times 10^4$  yr and  $1.036 \times 10^5$  yr after the merger. The time of the merger is defined as the time at which the two density peaks associated with the merging galactic cores are no longer distinguishable. For reference, the disk orbital time at  $\sim 20$  pc is  $5 \times 10^4$  yr, while at 1 pc it is  $\sim 4 \times 10^3$  yr. Global spiral modes, in particular the two-armed spiral initially triggered by the final collision between the two cores, are evident at scales of tens of parsecs (upper panels) and cause the mass increase in the central parsec region (bottom panels (a)-(b)) that allows the collapse into a massive central cloud (from bottom panel (b) to bottom panel (c)).

consistent with that inferred for the hosts of high-redshift quasars based on their number densities<sup>5,25</sup>. The two galaxies are placed on a parabolic orbit whose parameters are consistent with those found in cosmological simulations<sup>23,24</sup>. We employ the technique of smoothed particle hydrodynamics (SPH) to model the galaxy collision, including radiative cooling, star formation and a temperature floor at  $2 \times 10^4$  K to mimic non-thermal pressure due to turbulence in the interstellar medium (ISM) (see Supplementary Information).

The two merging galaxies undergo two close encounters as dynamical friction against their extended halos erodes their orbital energy. At the time when the two baryonic cores are separated by 6 kpc, when they begin their last orbit before the final collision, we perform particle splitting in the gas component within a volume 30 kpc in size (See Supplementary Information). As a result, we increase our gas mass resolution eight-fold and, simultaneously, we decrease the gravitational softening achieving a spatial resolution of 0.1 pc (see Supplementary Information). In this refined calculation we adopt an effective equation of state (EOS) that accounts for the net balance between cooling and heating<sup>26</sup>. A lower resolution un-refined simulation shows that during the final collision the star formation peaks at  $\sim 30 M_{\odot}/\text{yr}$  over about  $10^8 \text{yr}$ <sup>23</sup>. Motivated by this, we chose an EOS with an effective  $\gamma$  in the range 1.1 – 1.4 which is appropriate for interstellar gas heated by a major starburst<sup>27</sup> and assuming solar metallicity as suggested by the abundance analysis of the high-redshift QSOs<sup>22</sup> (see Supplementary Information).

The final collision of the two galactic cores produces a massive turbulent rotating nuclear disk with a mass of  $\sim 2 \times 10^9 M_{\odot}$  and a radius of about 80 pc<sup>24</sup>. With the increased resolution we can follow the internal evolution of the nuclear disk. The disk is born in an unstable configuration, with a prominent two-armed spiral pattern imprinted by the collision and sustained by its own strong self-gravity (Figure 1). The gas has a high turbulent velocity dispersion ( $\sigma \sim 100$  km/s) maintained by gravitational instability<sup>18</sup> and rotates at a speed of several hundred km/s within 50 pc. It constitutes most of the mass in the nuclear region, the rest being in dark matter and stars. The spiral arms swiftly transport mass inward and angular momentum outward<sup>28</sup>. About only  $10^4$  yr after the merger is completed, more than 20% of the disk mass ( $> \sim 5 \times 10^8 M_{\odot}$ ) resides within the central few parsecs (Figure 2) where the inflow rate peaks at  $\dot{M} > 10^4 M_{\odot}/\text{yr}$  (see Figure 1 of Supplementary Information) This corresponds to an inflow timescale  $t_{\text{inf}} = M/\dot{M} < T_{\text{orb}}$ , where  $T_{\text{orb}}$  is the local orbital timescale. The inflow rate is orders of magnitude higher than that expected in isolated, thin locally gravitationally unstable disks considered in analytic models of direct massive black hole formation<sup>16</sup>, but it is consistent with results of three-dimensional simulations of disks subject to global instabilities<sup>18,28</sup> (see Supplementary Information). The self-gravitating nuclear disk does not fragment because of its high effective thermal pressure and even higher turbulent pressure, which maintain a Toomre Q parameter above the threshold for stability (see Supplementary Information).

The gas funnelled to the central 2-3 pc region of the nuclear disk settles into a rotating, pressure supported cloud. The density of the cloud continuously increases as it gains mass from the inflow until it becomes Jeans unstable and collapses to sub-parsec scales on the

local dynamical time,  $t_{\text{dyn}} \sim 10^3$  yr (Figure 1). The supermassive cloud contains  $\sim 13\%$  of the disk mass ( $\sim 2.6 \times 10^8 M_{\odot}$ ) (Figure 2). The simulation is stopped once the central cloud has contracted to a size comparable to the spatial resolution limit. At this point the cloud is still Jeans unstable. With greater resolution its collapse should continue since the equation of state would become essentially isothermal at even higher densities<sup>27</sup>. With its steep density profile ( $r \sim \rho^{-\gamma}$ , with  $\gamma > 2$ ) the cloud would be very massive and dense even at much smaller radii. At a radius  $\sim 10^{-3}$  pc it would match the conditions of a quasi-star that can then collapse directly into a massive black hole<sup>9,10</sup>. Alternatively, it could collapse on a free-fall timescale into a massive black hole without prior formation of a quasi-star. Only  $\sim 10^5$  yr have elapsed since the completion of the merger, a timescale much shorter than the  $10^8$  years needed to convert most of the nuclear gas into stars during the starburst (see Supplementary Information). Therefore, in our merger simulation the gas flows inward and collapses into a compact object much faster than it can form stars, overcoming the major difficulty of previous direct formation models appealing to metal-free conditions in protogalaxies to suppress star formation<sup>10,16</sup>.

The very high temperature of the cloud,  $T > 10^7$  K, makes star formation in its interior highly unlikely. Yet, even if less than 1% of the cloud mass collapsed into a black hole it would still produce an object of mass  $> 10^5 M_{\odot}$  which can subsequently grow by accreting the surrounding nuclear gas disk (see Supplementary Information). Assuming that the disk forms stars with a  $\sim 30\%$  efficiency, as deduced from observation and models of star forming molecular clouds<sup>27</sup>, a gas mass in excess of  $10^9 M_{\odot}$  would still be available to feed the black hole over a timescale longer than  $10^8$  yr, the duration of the starburst. Considering Eddington-limited accretion<sup>29</sup> the black hole can grow to  $M_{\text{BH}} \sim 10^9 M_{\odot}$  in as little as  $3.6 \times 10^8$  yr (see Supplementary Information). Therefore the massive seed black hole can grow fast enough for bright quasars to arise within the first billion year from the Big Bang, namely by  $z \sim 6$ . This provided that the galaxy merger also occurs on a timescale shorter than a billion year, a natural condition in CDM models at high redshift due to the high densities and short orbital timescales of collapsed objects<sup>30</sup> (see Supplementary Information).

Large deviations from the local  $M_{\text{BH}} - \sigma$  relation (where  $\sigma$  is the velocity dispersion of the central stellar spheroid)<sup>22</sup> should be expected at high redshift as the black hole mass grows faster than that of its host galaxy. A black hole mass much larger than that inferred from the local  $M_{\text{BH}} - \sigma$  relation has actually been suggested for the only high-redshift quasar for which gas kinematics has been measured<sup>25</sup>. Substantial evolution in the high-redshift scaling relations between SMBHs and their host galaxies will be testable with future observations of bright quasar hosts with the James Webb Space Telescope (JWST) and the Atacama Large Millimeter Array (ALMA). At low redshift the formation mechanism that we propose should be suppressed as pre-existing SMBHs in the two merging galaxies heat the surrounding medium while they accrete gas, preventing instabilities and inflows in the nuclear disk. Finally, future gravitational wave experiments such as the Laser Interferometer Space Antenna (LISA) will be able to test the existence of a population of

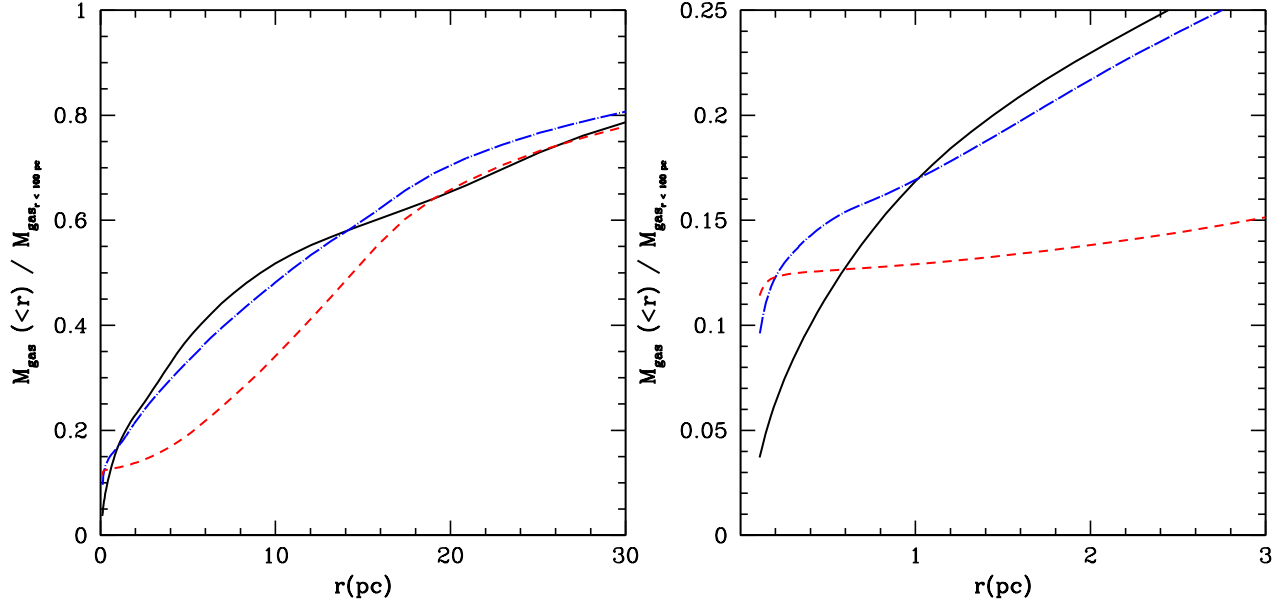


**Figure 2. Evolution of the cumulative gas mass profile of the nuclear disk.** Profiles are normalized to the total gas mass within the radius the nuclear disk (100 pc). The disk radius is determined from the sharp drop in the nuclear gas density distribution. The left panel shows the profile at scales of tens of parsecs, while the right panel displays the profile within the inner few parsecs. In both panels different curves show the mass profile at  $9.1 \times 10^3$  yr (solid line),  $7.49 \times 10^4$  yr (dot-dashed line) and  $1.036 \times 10^5$  yr (dashed line) after the merger, these being the same snapshots used in Figure 1. The time of the merger is defined as the time at which the two density peaks associated with the merging cores of the galaxies are no longer distinguishable. Mass redistribution is evident as spiral arms at tens of parsecs scales push mass inward and shed angular momentum outwards (top panel), gradually leading to an increasing mass concentration in the central region (bottom panel). This triggers the Jeans collapse of the central inner few parsecs into a supercloud containing  $\sim 13\%$  of the total disk mass, which manifests as a strong flattening of the profile at parsec scales as the cloud absorbs a large fraction of the mass in that region

black holes that had a jump start by probing the mass distribution of merging black holes as a function of redshift .

---

Received 22 December 2009; Accepted **draft**.

1. Fan, X, Evolution of high redshift quasars, *New AR*, **50**, 665-671 (2006)
2. Madau, P., & Rees, M.J., Massive Black Holes as Population III Remnants *Astrophys. J.*, **551**, L27-L30 (2001)
3. Volonteri, M., & Rees, M.J., Quasars at  $z=6$ : The Survival of the Fittest, *Astrophys. J.*, **650**, 669-678 (2006)
4. Johnson, J.L., & Bromm, V, The aftermath of the first stars: massive black holes *Mon. Not. R. Astron. Soc.*, **474**, 1557-1568 (2007)
5. Pelupessy, F.I., di Matteo, T., & Ciardi, B., How Rapidly Do Supermassive Black Hole “Seeds” Grow at Early Times? *Astrophys. J.*, bf 665, 107-119 (2007)
6. Alvarez, M.A., Wise, J.H., & Abel, T, Accretion onto the First Stellar Mass Black Holes, *Astrophys. J.*, submitted (2008)
7. Begelman, M., Volonteri, M., & Rees, M.J., Formation of supermassive black holes by direct collapse in pre-galactic halos, *Mon. Not. R. Astron. Soc.*, **370**, 289-298 (2006)
8. Volonteri, M., Lodato, G., & Natarayan, The evolution of massive black hole seeds *Mon. Not. R. Astron. Soc.*, **383**, 1079-1088 (2008)
9. Begelman, M., Did Supermassive Black Holes Form by Direct Collapse?, *AIPC*, **990**, 489-493 (2008)
10. Omukai, K., Schneider, R., & Haiman, Z., Can Supermassive Black Holes Form in Metal-Enriched High Redshift Protogalaxies? *Astrophys. J.*, **686**, 801-814 (2008)
11. Bromm, V, & Loeb, A., Formation of the first supermassive black holes *Astrophys. J.* **596**, 34-36 (2003)
12. Milosavljevic, M., Couch, S. M., & Bromm, V., Accretion Onto Intermediate-Mass Black Holes in Dense Protogalactic Clouds, *Astrophys. J.*, **696**, L146-L149 (2009)
13. Haiman, Z., Constraints from Gravitational Recoil on the Growth of Supermassive Black Holes at High Redshift, *Astrophys. J.*, **613**, 36-40 (2004)
14. Haehnelt, M.G., Natarayan, P., & Rees, M.J., High-redshift galaxies, their active nuclei and central black holes *Mon. Not. R. Astron. Soc.*, **300**, 817-827 (1998)
15. Shlosman, J., Frenk, J, & Begelman, M.C., Bars within bars - A mechanism for fueling galactic nuclei *Nature*, **338**, 45-47 (1989)
16. Lodato, G, & Natarayan, P., Supermassive black hole formation during the assembly of pre-galactic discs, *Mon. Not. R. Astron. Soc.* **371**, 1813-1823 (2006)

17. Levine, R., Gnedin, N., Hamilton, A.J.S., & Kravtsov, *Astrophys. J.*, Resolving Gas Dynamics in the Circumnuclear Region of a Disk Galaxy in a Cosmological Simulation, **678**, 154-167, (2008)
  18. Wada, K., & Norman, C., Obscuring Material Around Seyfert Nuclei with Starbursts, *Astrophys. J.*, **566**, L21-L24 (2002)
  19. Escala, A., *Astrophys. J.*, Toward a Comprehensive Fueling-controlled Theory of the Growth of Massive Black Holes and Host Spheroids, **671**, 1264-1271 (2007)
  20. Balbus, S., & Hawley, J.F., A powerful local shear instability in weakly magnetized disks. I - Linear analysis. II - Nonlinear evolution. *Rev. Mod. Phys.*, **70**, 214-233 (1991)
  21. Eisenstein, D., & Loeb, A., Origin of quasar progenitors from the collapse of low-spin cosmological perturbations *Astrophys. J.*, **443**, 11-17 (1995)
  22. Djorgovski, S. G, Volonteri, M., Springel, V., Bromm, V. & Meylan, G. The Origins and the Early Evolution of Quasars and Supermassive Black Holes, Proc. XI Marcel Grossmann Meeting on General Relativity, eds. H. Kleinert, R.T. Jantzen & R. Ruffini, Singapore: World Scientific (2008)
  23. Kazantzidis, S., Mayer, L., Colpi, M., Madau, P., Quinn, T., Debattista, V., Wadsley, J. & Moore, B., The Fate of Supermassive Black Holes and the Evolution of the MBH- Relation in Merging Galaxies: The Effect of Gaseous Dissipation *Astrophys. J.* **623**, L67-L70 (2005)
  24. Mayer, L., Kazantzidis, S., Madau, P., Colpi, M., Quinn, T., & Wadsley, J., Rapid Formation of Supermassive Black Hole Binaries in Galaxy Mergers with Gas, *Science*, **316**, 1874-1877 (2007)
  25. Walter, F., Carilli, C., Bertoldi, F., Menten, K., Cox, P, Lo, K. Y., Fan, X., Strauss, M.A. Resolved Molecular Gas in a Quasar Host Galaxy at Redshift  $z=6.42$ , *Astrophys. J.* **615**, L17-L20 (2004)
  26. Spaans, M. & Silk, J., The Polytropic Equation of State of Interstellar Gas Clouds, *Astrophys. J.*, **538**, 115-120 (2000)
  27. Klessen, R.S., Spaans, M., Jappsen, A., The stellar mass spectrum in warm and dusty gas: deviations from Salpeter in the Galactic centre and in circumnuclear starburst regions, *Mon. Not. R. Astron. Soc.*, **374**, L29-L33 (2007)
  28. Krumholz, M. R., Klein, R. I., McKee, C. F. Radiation-Hydrodynamic Simulations of Collapse and Fragmentation in Massive Protostellar Cores. *Astrophys. J.*, **656**, 959-979 (2007)
  29. Shapiro, S.L., *Astrophys. J.*, Spin, Accretion, and the Cosmological Growth of Supermassive Black Holes **620**, 59-68 (2005)
  30. Mo, H, Mao, S., & White, S.D.M. The formation of galactic discs, *Astrophys. J.*, **295**, 319-336 (1998)
-



## **Acknowledgements**

Stimulating discussions with Monica Colpi, Richard Durisen, Fabio Governato, Piero Madau, Thomas Quinn, David Weinberg, Romain Teyssier and Simon White are greatly acknowledged. This research has been supported by the Swiss National Science Foundation (SNF), by the Center for Cosmology and Astro Particle Physics (CCAPP) at Ohio State University, and by the Kavli Institute for Particle Astrophysics (KIPAC) at Stanford University. LM, SK and SC acknowledge the Kavli Institute for Theoretical Physics at the University of California in Santa Barbara (KITP) for hospitality during the initial stages of this work during the program “Building the Milky Way”. All computations were performed on the Zbox3 supercomputer at the University of Zürich and on the Brutus cluster at ETH Zürich.

**Author Information** The authors declare that they have no competing financial interests. Correspondence and requests for materials should be addressed to L.M. (lucio@phys.ethz.ch) or S.K. (stelios@mps.ohio-state.edu).

## SUPPLEMENTARY INFORMATION

Here we briefly describe the setup of the initial conditions and the numerical methods used to perform the simulations presented in the Letter. This is followed by a critical discussion of the assumptions behind the modeling of thermodynamics in the simulations and by a quantitative discussion of the instability and dynamics of the nuclear disk to support the results described in this Letter. We conclude with a discussion of the growth of the massive black hole seed using analytical estimates.

### 1 Numerical Methods

#### 1.1 The N-Body+SPH code:GASOLINE

We have used the fully parallel, N-Body+smoothed particle hydrodynamics (SPH) code GASOLINE to compute the evolution of both the collisionless and dissipative component in the simulations. A detailed description of the code is available in the literature<sup>1</sup>. Here we recall its essential features. GASOLINE computes gravitational forces using a tree-code<sup>2</sup> that employs multipole expansions to approximate the gravitational acceleration on each particle. A tree is built with each node storing its multipole moments. Each node is recursively divided into smaller subvolumes until the final leaf nodes are reached. Starting from the root node and moving level by level toward the leaves of the tree, we obtain a progressively more detailed representation of the underlying mass distribution. In calculating the force on a particle, we can tolerate a cruder representation of the more distant particles leading to an  $O(N \log N)$  method. Since we only need a crude representation for distant mass, the concept of “computational locality” translates directly to spatial locality and leads to a natural domain decomposition. Time integration is carried out using the leapfrog method, which is a second-order symplectic integrator requiring only one costly force evaluation per timestep and only one copy of the physical state of the system.

SPH is a technique of using particles to integrate fluid elements representing gas<sup>3,4</sup>. GASOLINE is fully Lagrangian, spatially and temporally adaptive and efficient for large  $N$ . It employs radiative cooling in the galaxy merger simulation used as a starting point for the refined simulations presented in this Letter. We use a standard cooling function for a primordial mixture of atomic hydrogen and helium. We shut off radiative cooling at temperatures below  $2 \times 10^4$  K that is about a factor of 2 higher than the temperature at which atomic radiative cooling would drop sharply due to the adopted cooling function. With this choice we take into account non-thermal, turbulent pressure to model the warm ISM of a real galaxy<sup>5</sup>. Unless strong shocks occur (this will be the case during the final stage of the merger) the gaseous disk evolves nearly isothermally since radiative cooling is very efficient at these densities ( $< 100$  atoms/cm<sup>3</sup>) and temperatures ( $10^4$  K), and thus dissipates rapidly the compressional heating resulting from the non-axisymmetric structures (spiral arms, bars) that soon develop in each galaxy as a result of self-gravity and the

tidal disturbance of the companion. The cooling rate would increase with the inclusion of metal lines, but it has been shown (see section 1.4) that the equation of state of gas at these densities is still nearly isothermal ( $\gamma \sim 0.9 - 1.1$ ) for a range of metallicities (with  $\gamma$  being lower for higher metallicity), supporting the validity of our simple choice for the cooling function. Cooling by metals will surely be important below  $10^4$  K, but this would be irrelevant in our scheme since we have imposed a temperature floor of  $2 \times 10^4$  K to account for non-thermal pressure (see above). The specific internal energy of the gas is integrated using the asymmetric formulation. With this formulation the total energy is conserved exactly (unless physical dissipation due to cooling processes is included) and entropy is closely conserved away from shocks, which makes it similar to alternative entropy integration approaches<sup>6</sup>. Dissipation in shocks is modeled using the quadratic term of the standard Monaghan artificial viscosity<sup>4</sup>. The Balsara correction term is used to reduce unwanted shear viscosity<sup>7</sup>. The galaxy merger simulation<sup>8</sup> includes star formation as well. The star formation algorithm is such that gas particles in dense, cold Jeans unstable regions and in convergent flows spawn star particles at a rate proportional to the local dynamical time<sup>9,10</sup>. The star formation efficiency was set to 0.1, which yields a star formation rate of  $1-2M_{\odot}/\text{yr}$  for models in isolation that have a disk gas mass and surface density comparable to those of the Milky Way.

## 1.2 The simulations of galaxy mergers

For the Letter we performed a refined calculation of a galaxy merger simulation between two identical galaxies. The initial conditions of this and other similar merger simulations are described in previous papers<sup>8,9</sup>. The models are based on our knowledge of present-day disk galaxies simply because there is little information available from observations of galaxy structure at high redshift. Yet, this modeling strategy should be regarded as conservative for the purpose of this paper since high redshift disks are denser, more gas-rich and more turbulent than present-day galaxies, which should favour the formation of massive nuclear disks and, subsequently, of large gas concentrations within them. We employed a multi-component galaxy model constructed using the technique originally developed in<sup>11,12</sup>, its structural parameters being consistent with the  $\Lambda$ CDM paradigm for structure formation<sup>13</sup>. The model comprises a spherical and isotropic Navarro-Frenk-and-White (NFW) dark matter (DM) halo<sup>14,15</sup>, an exponential disk, and a spherical, non-rotating bulge. We adopted parameters from the Milky Way model A1 of<sup>16</sup>. Specifically, the DM halo has a virial mass of  $M_{\text{vir}} = 10^{12}M_{\odot}$ , a concentration parameter of  $c = 12$ , and a dimensionless spin parameter of  $\lambda = 0.031$ . The mass, thickness and resulting scale length of the disk are  $M_{\text{d}} = 0.04M_{\text{vir}}$ ,  $z_0 = 0.1R_{\text{d}}$ , and  $R_{\text{d}} = 3.5$  kpc, respectively. The bulge mass and scale radius are  $M_{\text{b}} = 0.008M_{\text{vir}}$  and  $a = 0.2R_{\text{d}}$ , respectively. While a stellar bulge is always present in the most massive disk galaxies out to  $z = 1$ <sup>17</sup> there is still insufficient knowledge of galactic structure at higher redshift to confirm that this is the case also at  $z > 6$ . However, the presence of the bulge has the effect of stabilizing the galaxy disks against external perturbations<sup>18</sup>. This implies that, without the bulge, the two disks would undergo even

stronger non-axisymmetric distortions during the final stage of the merger and initiate a gas inflow even more powerful than the one obtained in our current calculation. Hence including the bulge should be regarded as a conservative assumption for the purpose of this Letter.

The DM halo was adiabatically contracted to respond to the growth of the disk and bulge<sup>19</sup> resulting in a model with a central total density slope close to isothermal. The galaxies are consistent with the stellar mass Tully-Fisher and size-mass relations. The gas fraction,  $f_g$ , is 10% of the total disk mass. This is fairly typical for Milky Way-sized galaxies at low redshift but it is a conservative assumption for galaxies at  $z > 2$ <sup>20</sup>. The rotation curve of the model is shown in Figure 1. The simulation presented in this Letter is the refined version of a coplanar prograde encounter. This particular choice is by no means special for our purpose, except that the galaxies merge slightly faster than in the other cases, thus minimizing the computational time invested in the expensive refined simulation. In particular, in previous work we have shown that the existence of a coherent nuclear disk after the merger is a general result that does not depend on the details of the initial orbital configuration, including the initial relative inclination of the two galaxies<sup>8,9</sup>. Similarly, gas masses and densities in the nuclear region were found to differ by less than a factor of 2 for runs having the same initial gas mass fraction in the galaxy disks but different initial orbits.

The galaxies approach each other on parabolic orbits with pericentric distances that were 20% of the galaxy's virial radius, typical of cosmological mergers<sup>21</sup>. The initial separation of the halo centers was twice their virial radii and their initial relative velocity was determined from the corresponding Keplerian orbit of two point masses. Each galaxy consists of  $10^5$  stellar disk particles,  $10^5$  bulge particles, and  $10^6$  DM particles. The gas component was represented by  $10^5$  particles. We adopted a gravitational softening of  $\epsilon = 0.1$  kpc for both the DM and baryonic particles of the galaxy.

### 1.3 The refined simulations of the nuclear region

#### 1.3.1 Particle splitting

In this Letter we use the same technique of static particle splitting that has been used before to study the dynamics of supermassive black hole binaries evolving in circumnuclear gaseous disks<sup>22</sup> as well as during galaxy mergers<sup>8</sup>, and to study the assembly of galaxies from the cooling flow in a galaxy-sized halo<sup>23</sup>. A similar technique has been used by others to study the dynamics of binary black holes in spherical gaseous backgrounds<sup>24</sup>. In dynamic splitting the mass resolution is increased during the simulation based on some criterion, such as the local Jeans length of the system. This requires extreme care when calculating SPH density or pressure at the boundary between the fine grained and the coarse grained volumes<sup>25</sup>. In static splitting, the approach is much more conservative and one simply selects a subvolume to refine. The simulation is then restarted with increased mass resolution just in the region

of interest. By selecting a large enough volume for the fine grained region one can avoid dealing with spurious effects at the coarse/fine boundary. We select the volume of the fine-grained region large enough to guarantee that the dynamical timescale of the entire coarse-grained region is much longer than the dynamical timescale of the refined region. In other words, we make sure that gas particles from the coarse region will reach the fine region on a timescale longer than the actual time span probed in this work. This is important because the more massive gas particles from the coarse region can exchange energy with the lower mass particles of the refined region via two-body encounters, artificially affecting their dynamics and thermodynamics<sup>26</sup>. Hence our choice to split in a volume of 30 kpc in radius, while the two galaxy cores are separated by only 6 kpc. The new particles are randomly distributed according to the SPH smoothing kernel within a volume of size  $\sim h_p^3$ , where  $h_p$  is the smoothing length of the parent particle. The velocities of the child particles are equal to those of their parent particle (ensuring momentum conservation) and so is their temperature, while each child particle is assigned a mass equal to  $1/N_{\text{split}}$  the mass of the parent particle, where  $N_{\text{split}}$  is the number of child particles per parent particle. The mass resolution in the gas component was originally  $2 \times 10^4 M_\odot$  and becomes  $\sim 3000 M_\odot$  after splitting, for a total of 1.5 million SPH particles.. The star and dark matter particles are not splitted to limit the computational burden. The softening of the gas particles is reduced to 0.1 pc (it was 100 pc in the low resolution simulations). For the new mass resolution, the local Jeans length is always resolved by 10 or more SPH smoothing kernels<sup>27,28</sup> in the highest density regions occurring in the simulations.

The softening of dark matter and star particles remains 100 pc because these are not splitted. Therefore in the refined simulations stars and dark matter particles essentially provide a smooth background potential to avoid spurious two-body heating against the much lighter gas particles, while the computation focuses on the gas component which dominates by mass in the nuclear region. By performing numerical tests we have verified that, owing to the fact that gas dominates the mass and dynamics of the nuclear region, the large softening adopted for the dark matter particles does not affect significantly the density profile of the inner dark halo that surrounds the nuclear disk.

#### 1.4 Thermodynamics of the nuclear region

**Model description** In the refined simulations the gas is ideal and each gas particle obeys  $P = (\gamma - 1)\rho u$ . The specific internal energy  $u$  evolves with time as a result of  $PdV$  work and shock heating modeled via the standard Monaghan artificial viscosity term (no explicit radiative cooling term is included).

The entropy of the system increases as a result of shocks. Including irreversible heating from shocks is important in these simulations since the two galaxy cores undergo a violent collision. Shocks are generated even later as the nuclear, self-gravitating disk becomes non-axisymmetric, developing strong spiral arms. Therefore the highly dynamical regime modeled here is much different from that considered by previous works starting from an

equilibrium disk model, which could be evolved using a polytropic equation of state and neglecting shock heating<sup>22,29</sup>. Radiative cooling is not directly included in the refined simulations. Instead, the magnitude of the adiabatic index, namely the ratio between specific heats, is changed in order to mimic different degrees of dissipation in the gas component, thereby turning the equation of state of the gas into an “effective” equation of state<sup>30,31</sup>. We have shown elsewhere<sup>9</sup> that the transition between the radiative cooling regime and the effective equation of state regime does not introduce numerical artifacts in the simulation.

Previous works<sup>31</sup> have used a two-dimensional radiative transfer code to study the effective equation of state of interstellar clouds exposed to the intense UV radiation field expected in a starburst finding that the gas has an adiabatic index  $\gamma$  in the range 1.1–1.4(= 7/5) for densities in the range  $5 \times 10^3 - 10^5$  atoms/cm<sup>3</sup>, comparable to the volume-weighted mean density in the simulated nuclear disk. Such values of the adiabatic index are expected for quite a range of starburst intensities, from  $10 M_\odot/\text{yr}$  to more than  $100 M_\odot/\text{yr}$ , hence encompassing the peak star formation rate of  $\sim 30 M_\odot/\text{yr}$  measured in the original low-res galaxy merger simulations<sup>8</sup>. Hence under these conditions the nuclear gas is not isothermal ( $\gamma = 1$ ), which would correspond to radiative cooling being so efficient to balance heating coming from compression and/or radiative processes, as it happens in the first stage of the simulation. Its inefficient cooling at densities of  $10^4$  atoms/cm<sup>3</sup> is mostly due to a high optical depth which causes trapping in H<sub>2</sub>O and CO lines. In addition the warm dust heated by the starburst continuously heats the gas via dust-gas collisions, and the cosmic-rays do so as well<sup>31</sup>. We adopt  $\gamma = 7/5$  until the first gas inflow is completed in the simulation (we have also run a case for  $\gamma = 1.3$  and found that the structure of the nuclear disk is substantially unchanged). That the mean properties (mass, density, pressure support contributed by the thermal and turbulent components, rotational velocity) of nuclear disks formed in galaxy mergers<sup>32</sup> and simulated with such an effective equation of state compare well with the corresponding properties of nuclear disks observed in detailed observations of merger remnants has been already shown in previous work<sup>9</sup>. For densities above  $10^5$  atoms/cm<sup>3</sup> cooling is more efficient and  $\gamma$  should drop to  $\sim 1.1$  according to the adopted EOS model<sup>31</sup>. This condition is verified in the central few parsecs after the first inflow ( $\sim 10^4$  yr after the merger), hence  $\gamma = 1.1$  is adopted from this time onward. By comparing with another simulation that was continued with  $\gamma = 1.4$  we verified that the dynamics of the disks at larger scales (tens of parsec scales) are not affected by varying  $\gamma$ .

With our EOS we model the nuclear gas as a one-phase medium. In reality the nuclear disks will have a complex multi-phase structure with temperatures and densities spanning orders of magnitude even in localized regions, as shown by detailed numerical calculations of nuclear disk models<sup>33,34</sup>. In particular, even the same radius the disk may have regions with different densities that may evolve as if the equation of state was varying locally. Furthermore, based on the assumed EOS model<sup>31</sup> the lowest density ( $< 10^3$  atoms/cm<sup>3</sup>) and highest density gas ( $> 10^6$  atoms/cm<sup>3</sup>) is characterized by an adiabatic index  $\gamma \leq 1$ , hence by a lower sound speed  $v_s = \sqrt{\gamma k_B T / \mu}$ . A lower gas sound speed will make the disk

more gravitationally unstable, lowering the Toomre Q parameter, and thus more prone to fragmentation and star formation<sup>35</sup>. However, as the Toomre parameter is lowered stronger asymmetries and spiral modes will also occur, increasing the gas inflow. The question is then whether the net amount of mass transported to the center will also increase or will be reduced by the competing effect of star formation. Recent numerical work<sup>36</sup> has shown that even with specific star formation rates 5 times higher than expected based on the Kennicutt-Schmidt law gas inflows are still prominent and lead to a significant deposition of mass to the center of an isolated rotating nuclear gas disk model, strongly suggesting that the results presented in this Letter will remain valid even in a more realistic calculation incorporating star formation and local variations of the effective equation of state.

**Star formation and feedback** The conversion of gas into stars is not included in the refined calculation with particle splitting presented in this Letter, although its (important) radiative feedback effect on gas thermodynamics is included with the choice of the EOS (see previous subsection). Indeed the refined calculation is carried out for less than 1% of the starburst duration of  $10^8$  yr indicated by the companion merger simulation carried out without splitting<sup>8,9</sup>, suggesting that the conversion of gas into stars is not important on the timescales of interest for this work. Cautionary remarks regarding this point are however necessary. Had we included star formation directly in the refined simulations we would have probably found local gas consumption timescales shorter than the global starburst timescale since with splitting much higher densities are resolved and the star formation rate depends on the local gas density. As for the first issue, we can obtain a rough estimate of how short the star formation timescale can be in the following way. To begin with, in the nuclear disk most of the gas is at densities above  $100 \text{ atoms/cm}^3$ . At these densities molecular hydrogen formation is efficient<sup>37</sup>. Let us then make the extreme assumption that all the gas in the disk is molecular and readily available for star formation. Then, let us simply assume that molecular gas will be turned into stars on the local orbital timescale. Star formation in molecular clouds is rather inefficient, and typically  $\leq 30\%$  of the dense, molecular gas is converted into stars, possibly because internal turbulence in the clouds prevents them from collapsing altogether<sup>35</sup>. Therefore let us write the star formation rate in the nuclear disk as a whole as  $dM_*/dt = 0.3 \times M_{gas}/T_{orb}$ , where  $T_{orb} = 2.5 \times 10^5$  years, the orbital time at the disk half mass radius, 25 pc, and  $M_{gas} = 3 \times 10^9 M_\odot$  is the mass of the enclosed mass of the disk at such distance. The resulting upper limit on the star formation rate is  $3600 M_\odot/\text{yr}$ , about 80 times higher than that estimated in the low-res simulations. Nonetheless, even with such high star formation rate only 10% of the gas within 25-30 pc (this is also the region where the first inflow occurs - see next section and Figure 1) would be converted into stars during the time required to form the central supermassive cloud ( $\sim 10^5$  years). On the other end, this high star formation rate justifies the use of the EOS valid for a starburst regime even on the short timescales probed by our calculations. These simple estimates suggest that our results should be qualitatively valid in general.

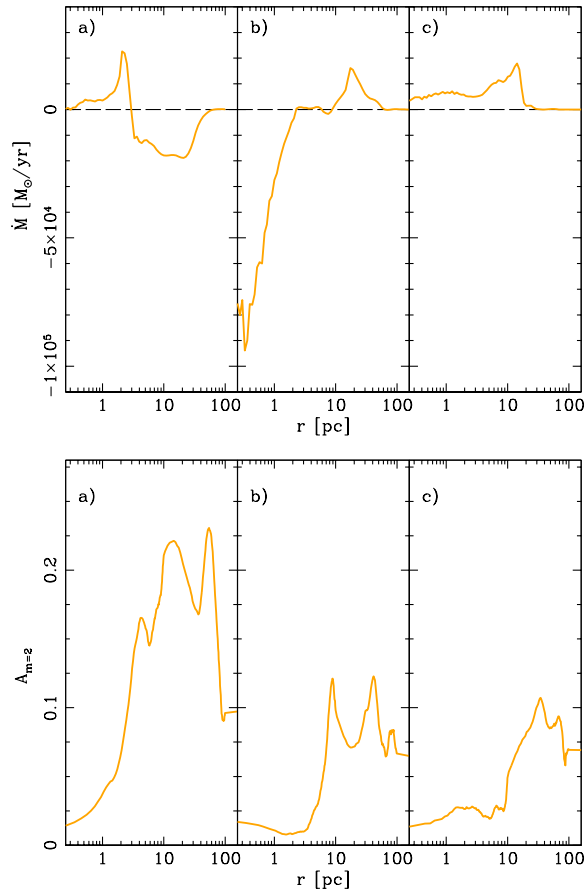


**Figure 3.** Time evolution of the gas inflow rate (top panel) and of the amplitude of the strongest non-axisymmetric mode in the disk (bottom panel,  $m = 2$  is the strongest mode at all times). Azimuthally averaged radial profiles are shown in both cases, time averaged over a few outputs around a chosen time  $t_*$  to avoid selecting transients. From left to right we show profiles at  $t_* = 9.1 \times 10^3$  yr (a),  $7.49 \times 10^4$  yr (b) and  $1.036 \times 10^5$  yr (c) after the merger, these being the same snapshots used in Figure 1 and 2 of the main paper. The time of the first snapshot (a) was indeed chosen near the maximum peak of the  $m = 2$  mode, which also corresponds to a maximum inflow rate at scales of  $\sim 10 - 20$  pc. At time (b) the Jeans collapse has already started at parsec scales, as shown by the very large inflow rate, which is indeed the highest measured throughout the simulation. At larger ( $\sim 10$  pc) scales the inflow has instead decreased because the dominant global  $m = 2$  mode has also weakened considerably (bottom panel). At time (c) the  $m = 2$  mode has faded considerably (higher order modes are now shown but they are even weaker at this time), the inner region is stable while outside the central parsec a net outflow is seen, which is responsible for the spreading of the disk highlighted in Figure 2 of the main paper.



Nonetheless, the arguments just outlined are based on simple scaling laws and, in particular, neglect the multi-phase nature of the ISM in the nuclear disks, that is important for star formation and is not accounted for in our EOS model. Furthermore, they are based on using average properties in the disk. In principle at radii of order a parsec or less higher densities and shorter dynamical times would yield higher star formation rates, potentially lowering the gas mass available to the central cloud. How much of the cloud mass would be lost to stars will also depend on the balance of heating and cooling *within the cloud*, which is beyond the reach of our resolution. However, as explained in the letter, the high temperature of the cloud,  $T > 10^7$  K, and the fact that further collapse should occur nearly isothermally as  $\gamma$  approaches unity at even higher densities, thus preserving such high temperatures, argue against the importance of star formation within the cloud. Nonetheless, the thermodynamics in the interior of the cloud in the later stages of the collapse is not necessarily captured by our EOS model (see <sup>38</sup> on the importance of the form of the EOS for fragmentation of gas clouds). For example, if a quasi-star forms at scales well below our resolution as a result of the collapse, only a small fraction of its mass would collapse instantaneously into a black hole, while the rest will be accreted at super-Eddington rates from the gaseous envelope of the quasi-star on timescales of  $10^5$  yr<sup>39</sup>. In this case there will be time for the rapidly growing seed black hole to affect the surrounding gas via radiative feedback, which would translate in a modification of the gas EOS and in a reduced efficiency in the growth of the massive seed. This is why we decided to be conservative and assumed that only 0.1% of the central gas cloud would end up into a black hole.

Along with star formation, another astrophysical aspect that we include in a very simplified way is feedback from star formation. Radiative feedback from stars is implicitly included in our choice of the effective equation of state (see above), but feedback from supernovae explosions is not taken into account. However, feedback from supernovae type II, would contribute to both heating the gas and increasing its turbulence (the timescale of supernovae type II explosions is sufficiently short to be relevant here), which should go in the direction of decreasing the star formation rate and therefore strengthening our previous argument concerning the role of star formation. It would also tend to stiffen the equation of state even in the central, high density regions, likely bringing our “mean” effective  $\gamma$  in closer agreement to the values adopted here. On the other end, a quick calculation suggests that feedback should not have a major impact on the global energetics of the nuclear disk. In fact, assuming the upper limit on the star formation rate of  $3600M_{\odot}/yr$  and a Miller-Scalo initial stellar mass function we obtain that supernovae should damp  $\leq 2.5 \times 10^{52}$  erg/yr ( $7 \times 10^{48}$  erg per solar mass of stars formed) into the surrounding gas, corresponding to  $\leq 2.5 \times 10^{57}$  erg damped during the black hole formation timescale,  $\sim 10^5$  yr. This is at most 20% of the the overall internal energy budget of the gas in the nuclear disk (the sum of turbulent, rotational and thermal energy), hence the effects on thermodynamics will be moderate. In addition most of this energy will be deposited outside the inner few parsecs since there the strong radial inflow will dominate over star formation because there the inflow timescale is shorter than the orbital timescale on which star formation proceeds. As

a result, the dynamics of the gas inflow, that are crucial in our formation model, should not be significantly affected.

**Feedback from the accreting massive seed black hole** Finally, once the black hole forms it will start accreting and will lose part of the accretion energy either radiatively or in part radiatively and in part in form of mechanical energy if a powerful jet is produced as observed in some of the local and distant AGNs. This is the so called "AGN feedback", whose effect we have not taken into account in the simple calculation of the timescale for the black hole to grow up to  $10^9 M_\odot$ . Indeed, based on recent calculations<sup>40</sup>, a SMBH starting with  $10^5 M_\odot$  should be able to accrete enough mass by  $z = 6$  even when the radiative feedback from black hole accretion (AGN feedback) is accounted for. Note that hydrodynamical effects and momentum deposition due to jets would deserve a separate discussion but are currently not well understood.

At low redshift two accreting SMBHs should be already present in the galaxies as they merge. Heating of the surrounding gas by "AGN feedback" might be strong enough to overcome cooling and produce a stiffer equation of state in the nuclear gas<sup>9</sup>. In this case, either a dense nuclear disk will not form at all<sup>9</sup>, and so no multi-scale scale gas inflows will occur, or the higher pressure support of the gas within the nuclear disk could prevent the secondary inflow and thus the formation of the central supermassive cloud.

## 2 Mass transport and stability of the nuclear region

We have measured the strength of the non-axisymmetric modes in the nuclear disk using a Fourier decomposition in order to establish a clear correlation between the regions of the disk at which the maximum inflow occurs in the nuclear disk and the amplitude of the strongest mode. This is shown in the panels of Figure 1. The strongest mode in the disk is at all times a two-armed spiral, corresponding to  $m = 2$  in the Fourier decomposition, as also apparent in Figure 1 (top panel) of the main paper. Such mode is the imprint of the collision between the two galaxy cores. The inflow rate is remarkable, peaking at  $> 10^4 M_\odot/\text{yr}$ , which corresponds to radial velocities of about 100 km/s. This is sustained for only a few  $10^4$  yr, allowing to bring a few  $10^8 M_\odot$  of gas within the inner 10 pc. Note that the large radial velocities are of order of the turbulent velocities seen in nuclear disks residing at the center of merger remnants<sup>32</sup>. In Figure 1 we also show the second radial inflow triggered by the onset of the Jeans collapse of the gas within the central parsec. The collapse begins at about a parsec scale as soon as the enclosed mass climbs above the local Jeans mass ( $\sim 7 \times 10^7 M_\odot$  at  $r = 1$  pc, note that using the Bonnor-Ebert mass would yield essentially the same result within a factor  $\sim 2$ ). Gas at about a parsec scale rotates at a speed of about  $v_{rot} \sim 600$  km/s but it is pressure supported as the temperature raises close to  $10^8$  K at such scales owing to adiabatic compression ( $v_s \sim 1000$  km/s  $> v_{rot}$ ). The fact that pressure provides the most important support against gravity justifies our use of the Jeans mass to characterize the phase of collapse, although a more complete description of

the process would involve accounting for the effect of rotation and the continued mass flux from the outer region of the disk.

We note that, owing to the high mass resolution reached after applying particle splitting, the local Jeans length is always well resolved throughout the disk, in the sense that it is about an order of magnitude larger than either the local SPH smoothing length or the gravitational softening<sup>27</sup>. The smoothing length is comparable with the softening at parsec scales, but becomes nearly an order of magnitude smaller than the latter when approaching a fraction of a parsec, suggesting that, if anything, the collapse may be slowed down once the cloud contracts to a size of order the softening. This implies that our conclusion that the inner supermassive cloud will continue to collapse further should be regarded as conservative; with greater resolution, indeed, not only the collapse should continue but should likely be faster.

The right snapshots of Figure 1 show the final expansion of the disk as the spiral arms unwind and transfer angular momentum outward of tens of parsecs, generating a net outflow. At this point the inner profile has reached stability as further collapse is not possible once the resolution limit is reached. Expansion of the disk as a result of angular momentum transfer driven by spiral modes is a well documented phenomenon in both gaseous and stellar disks from galactic to planetary scales<sup>41,42</sup>.

In Figure 2 we show the evolution of the Toomre parameter, which strictly measures the *local* stability of a differentially rotating disk to axisymmetric perturbations<sup>18</sup>. It is important to note that the disk is born out of equilibrium from the collision of the two cores, rather than becoming unstable starting from an equilibrium rotational configuration as assumed in the standard perturbative approach. The disk indeed reaches a near-equilibrium configuration after the phase of intense inflows studied in this paper. Nevertheless, previous studies on gaseous disks have shown that the Toomre parameter provides a good empirical measure of the susceptibility of disks to fragmentation quite irrespective of how the disk is initially set up, and in this sense also applies well to *global* stability to generic, non-axisymmetric perturbations<sup>43</sup>. The Figure shows that the Toomre parameter remains always in the theoretical regime of stability against fragmentation, although it drops initially to values in the range 1 – 1.5 where strong spiral instabilities are expected and are indeed observed. After the phase of strong non-axisymmetric instability associated with the inflow and subsequent central collapse is terminated (first and second panel) the disk self-regulates to a more stable state, with a minimum  $Q \sim 2$ .

It is instructive to compare the very high inflow rates measured in the nuclear disk with the expectations of analytical models that study a self-gravitating, thin isothermal accretion disk in steady state. Note that such models are based on a local stability analysis, in contrast with the global character of instability in our nuclear disk. Under such assumption, recent works argue that there exists maximum inflow rate in such a disk above which fragmentation, and thus star formation, will occur<sup>44,45</sup>. In steady state, the maximum inflow rate can be expressed as  $\dot{M}_{\max} = 2\alpha \frac{v_s^3}{G}$ , where  $\alpha \sim 0.06$  is the maximum disk viscosity, resulting from gravitational stresses,  $G$  is the gravitational constant, and  $v_s$  is the

sound speed. They consider protogalactic disks with temperatures  $\sim 4000$  K ( $v_s \sim 5$  km/s) for which  $\dot{M}_{\text{max}} = 10^{-2} M_{\odot}/\text{yr}$ . In our disks the thermal sound speed is much higher, but because the disks are in a gravoturbulent state, it is more sensible to consider the sum of the thermal sound speed and turbulent velocity dispersion, as we have done for the Toomre Q parameter (see Figure 2). This amounts to about  $600 - 700$  km/s at scales of 25 pc (the scale of the first inflow - see Figure 1), which implies an increase of a factor up to  $140^3 = 2.7 \times 10^6$ , which would yield a maximum inflow rate  $\sim 10^4 M_{\odot}/\text{yr}$ , quite in agreement with the results shown in Figure 1 (first panel). The second inflow at parsec scales is even higher and seems to overshoot the maximum rate possible without fragmentation, but since this is triggered by the Jeans collapse of the central cloud rather than by transport by spiral waves (see Figure 1) the argument based on the maximum viscous stress associated with gravitational instability does not apply anymore. In addition, the assumption of steady state, which is not appropriate in general under the highly dynamical conditions of our nuclear disk, clearly does not apply once the central cloud begins to collapse. As anticipated above, the analytical approach just outlined also stems from a local stability analysis of self-gravitating accretion disks<sup>36</sup>, while the gravoturbulent state of the nuclear disk is inherently related to the global character of the non-axisymmetric instability; in globally unstable disks "effective"  $\alpha$  viscosities even larger than unity can easily arise<sup>45</sup>. Dropping the constraint  $\alpha \sim 0.06$ , as suggested by the nature of global instability, would allow even higher inflow rates without fragmentation.

In any case, our simple analysis shows how a hot, gravoturbulent disk can easily sustain accretion rates orders of magnitude higher than those of cold, non-fragmenting protogalactic disks considered in recent literature, hence allowing naturally the formation of central supermassive objects without drainage of gas by star formation. These particular conditions arise naturally in the highly perturbed nuclear disk emerging from a galaxy merger, and should indeed be interpreted as a by product of the starburst itself. Thus, in our model star formation has indeed a positive role in allowing the direct collapse since it provides enough heating to prevent large-scale fragmentation.

Finally, typical galaxies at high redshift would have larger reservoirs of gas to form and feed the black hole relative to the initial conditions adopted in this Letter. Their more compact galactic disks (disk sizes are expected to scale as  $(1+z)^{-3/2}$  as their embedding dark halos in the CDM cosmogony, see also next section) would have produced more compact and dense gaseous nuclei after the merger, whose shorter dynamical timescales would drive an even faster mass transport towards the center via gravitational instabilities. Hence the results presented here should be regarded as conservative for the purpose of our scenario.

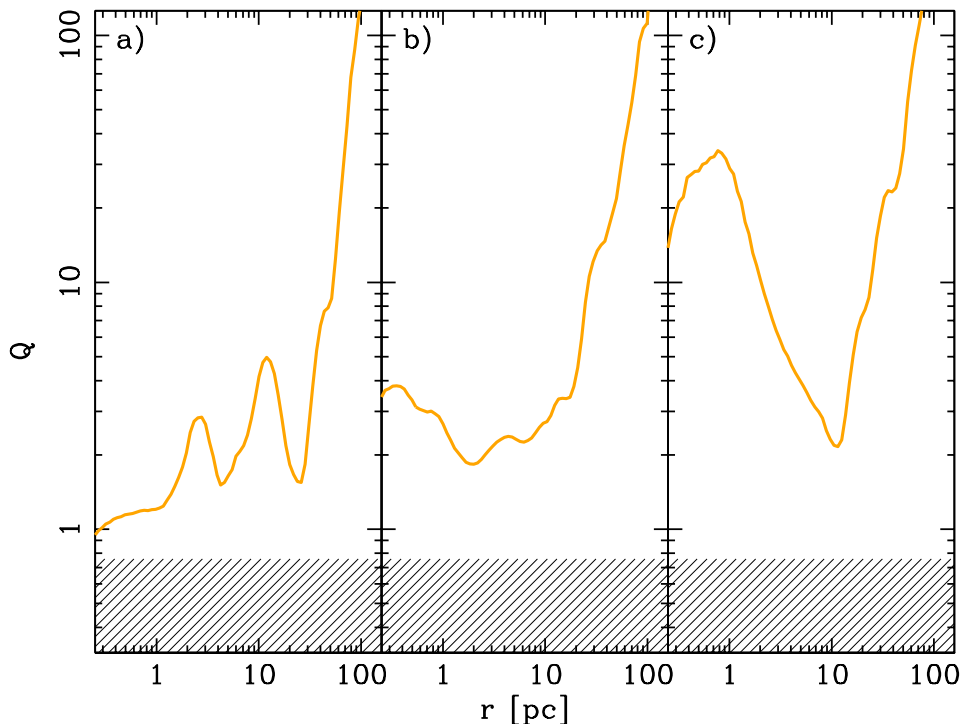


**Figure 4.** Azimuthally averaged Toomre  $Q$  profile of the disk shown at the same times as in Figure 1 (time increasing from left to right). The shaded area corresponds to the instability region marked by  $Q \leq 0.67$ , this being the stability threshold for finite thickness disks<sup>46</sup>. The Toomre parameter is calculated as  $Q = \kappa v_{s*} / \pi G \Sigma$ , where  $v_{s*}$  is the effective sound speed including the contribution of the turbulent (radial) velocity dispersion,  $v_{s*} = \sqrt{(v_s^2 + \sigma_r^2)}$ , where  $v_s$  is the thermal sound speed and  $\sigma_r$  the radial velocity dispersion of the gas. Note that  $\sigma_r \sim v_s$  outside the central few parsecs; within the inner few parsecs, especially after the onset of the Jeans collapse (panels b - c) the thermal pressure is dominant as the gas is strongly adiabatically compressed (the high central value of  $Q$  seen in panel (c) is associated with the formation of the supermassive hot central cloud).

### 3 Growth of the massive black hole seed

The time  $t(M_{\text{BH}})$  required for a black hole of initial mass  $m_{\text{seed}}$  to reach a mass  $M_{\text{BH}}$  assuming Eddington limited accretion<sup>47</sup> is given by  $t(M_{\text{BH}}) = \tau \times f_{\text{edd}}^{-1} \times \left(\frac{\epsilon_r}{1-\epsilon_r}\right) \times \ln(M_{\text{BH}}/m_{\text{seed}})$ , where  $M_{\text{BH}} = 10^9 M_{\odot}$ ,  $m_{\text{seed}} = 10^5 M_{\odot}$ ,  $f_{\text{edd}}$  expresses at which fraction of the Eddington limit the black hole is accreting, and  $\epsilon_r$  is the radiative efficiency. In our case  $M_{\text{BH}} = 10^9 M_{\odot}$  and  $m_{\text{seed}} = 2.6 \times 10^5 M_{\odot}$  (corresponding to 0.1% of the mass of the collapsing central cloud in our simulation). Furthermore, we choose standard parameters  $f_{\text{edd}} = 1$ ,  $\epsilon_r = 0.1$  and, to compute the characteristic accretion timescale  $\tau$ , we adopt a molecular weight per electron for a plasma at zero metallicity with cosmic abundance of hydrogen ( $X = 0.75$ ) and helium ( $Y = 0.25$ ),  $\mu_e = 1/(1 - Y/2) = 1.14$ , so that  $\tau = 0.45\mu_e^{-1} = 0.395$  Gyr. Note that metallicity effects are marginal in this calculation because they only have a negligible effect on the value of the molecular weight<sup>48</sup>. With these choices, we obtain  $t(M_{\text{BH}}) = 0.362$  Gyr. Assuming that the seed black hole can accrete at the Eddington limit ( $f_{\text{edd}} = 1$ ) is justified by the fact that the hole would accrete the gas belonging to the nuclear disk, which has very high densities  $n_H \sim 10^5 - 10^8$  atoms/cm<sup>4</sup> at scales below 10 pc. Such densities are several orders of magnitude higher than e.g. those of the gas surrounding the small black hole seeds formed by the collapse of Pop III stars, which accrete at sub-Eddington rates<sup>49</sup>. Therefore, not only our model can lead to seeds that are much more massive relative to those resulting from Pop III stars, but also the following gas accretion and growth occurs in a much more favourable environment.

Although we have adopted standard values of the parameters to calculate  $t(M_{\text{BH}})$  we can ask how much these can be varied while still being able to reach a billion solar masses within the first billion years. The timescale, due to its functional form, is especially sensitive to the radiative efficiency. Theoretically, the actual value of  $\epsilon_r$  depends on the spin of the black hole, which in turn depends on the uncertain mechanism of accretion, such as if the accretion occurs with or without magnetohydrodynamical (MHD) effects<sup>47</sup>. It may be as large as 0.42 for maximally spinning black holes<sup>47</sup> accreting in standard thin disks, in which case  $t(M_{\text{BH}})$  would exceed 1 Gyr. The timescale would instead be  $\sim 0.8$  Gyr for  $\epsilon_r = 0.2$ , as possible in MHD disks. It is important to stress that values of  $\epsilon_r$  in the range 0.1 – 0.2 should be regarded as more realistic since they are independently inferred from the ratio  $R$  of the QSO plus AGN luminosity density to the mass density of SMBHs in nearby galaxies<sup>50</sup>. In summary,  $t(M_{\text{BH}}) < 1$  Gyr requires  $\epsilon_r \leq 0.2$  and  $f_{\text{edd}} \geq 0.7$ . On the other end, if the galaxy merger occurs at  $z \sim 8$ , and the black hole has to grow to its final mass by  $z \sim 6$ , the time available for accretion is  $< 0.5$  Gyr for the standard WMAP5 cosmology, which then favours our standard choice of parameters  $f_{\text{edd}} = 1$  and  $\epsilon_r = 0.1$ .

As highlighted in the Letter, for the SMBHs to grow as required in the short time available it is also necessary that the merger timescale is significantly shorter than a billion year. Using simple scaling relations for galaxies and their halos in CDM models<sup>51</sup> one can show that, at a fixed virial mass  $M_{\text{vir}}$ , these are both smaller and denser compared to  $z = 0$ . This reflects the fact that the Universe itself is denser at higher redshift. This

reduces significantly the typical orbital time between pairs of collapsed objects, and thus the merging timescale, relative to  $z = 0$ . The orbital time during the merger (assuming for simplicity a circular orbit) is of order  $2\pi R_{vir}/V_c$ , where the halo circular velocity  $V_c$  and the virial radius  $R_{vir}$  at fixed  $M_{vir}$  increase and decrease, respectively, with increasing redshift. Using the standard scaling relations of Mo, Mao & White<sup>50</sup> for such quantities one can show that  $T_{orb} \sim (1+z)^{-3/2}$ . Since at  $z = 0$  the merging timescale on a typical cosmological orbit is  $\sim 5$  Gyr<sup>8</sup>, it follows that at  $z = 8$  this drops to  $\sim 0.2$  Gyr, which is comfortably shorter than a billion year.

Finally, in the conventional model in which light seed black holes originate from the collapse of Pop III stars their growth can be hampered if they are kicked out after merging with another hole due to the ‘gravitational rocket’ effect<sup>52</sup>. This phenomenon can have an important, negative impact on the growth of large black holes<sup>53</sup>. In our direct formation model two obvious scenarios are possible; either the black hole grows in a galaxy with no pre-existing hole, as we assumed throughout the paper, or it grows in galaxy where a light ‘Pop III seed’ hole is also present (this would have remained light due to inefficient accretion). In the first case the gravitational rocket is not important. In the second case, the lighter black hole could be kicked out of the galaxy, but since it would be orders of magnitude less massive it will not have an impact on the final mass growth of the primary black hole formed by direct collapse. In a third, less trivial scenario, the galaxy merger remnant could merge with a third, similarly massive galaxy in which another black hole has grown to a similarly large mass, after forming by direct collapse during a previous merger. In this case the gravitational rocket may be important since the two holes may have a similar (large) mass when they merge at the center of the remnant. However, the probability that this may happen before each black hole has reached a billion solar masses is quite low, since the merger timescale at  $z = 6 - 8$  is not smaller than the characteristic growth timescale of the black hole calculated with our standard parameters, rather is of the same order (see main paper). We conclude that, in general, kicks due to the gravitational rocket should not affect the conclusions of our work.

## References

1. Wadsley, J., Stadel, J., & Quinn, T., *New Astr.*, **9**, 137 (2004)
2. Barnes, J., & Hut, P., *Nature*, **324**, 446 (1986)
3. Gingold, R.A. & Monaghan, J.J., *Mon. Not. R. Astron. Soc.*, **181**, 375 (1977)
4. Monaghan, J.J., *Annual. Rev. Astron, Astrophys*, **30**, 543 (1992)
5. Barnes, J., *Mon. Not. R. Astron. Soc.*, **333**, 481 (2002)
6. Springel, V. and Hernquist, L., *Mon. Not. R. Astron. Soc.*, **333**, 649 (2002)

7. Balsara, D.S., *J.Comput. Phys.*,121, 357 (1995)
8. Kazantzidis, S., Mayer, L., Colpi, M., Madau, P., Debattista, V., Quinn, T., Wadsley, J. & Moore, B., *Astrophys. J.*, **623**, L67 (2005)
9. Mayer, L., Kazantzidis, S., Madau, P., Colpi, M., Quinn, T., & Wadsley, J., Rapid Formation of Supermassive Black Hole Binaries in Galaxy Mergers with Gas *Science*, **316**, 1874 (2007)
10. Katz, N. *Astrophys. J.*, **391**, 502 (1992)
11. Governato, F., Mayer, L., Wadsley, J., Gardner, J. P., Willman, B., Hayashi, E., Quinn, T., Stadel, J.& Lake, G, *Astrophys. J.*, **607**, 688 (2004)
12. Hernquist, L., *Astrophys. J. Supp.*, **86**, 389 (1993)
13. Springel, V. & White, S.D.M., *Mon. Not. R. Astron. Soc.*, **307**, 162 (1999)
14. Mo, H. J., Mao, S., White, S. D. M., *Mon. Not. R. Astron. Soc.*, **295**, 319 (1998)
15. Navarro, J. F., Frenk, C. S. & White, S. D. M., *Astrophys. J.*, **462**, 563 (1996)
16. Klypin A., Zhao H. & Somerville R. S., *Astrophys. J.*, **573**, 597 (2002)
17. Sargent, M.T., The Evolution of the Number Density of Large Disk Galaxies in COSMOS, *Astrophys. J. Supp.*, **162**, 434-455 (2007)
18. Binney, J., & Tremaine, S., Galactic Dynamics, Princeton University Press (1987, 2008)
19. Blumenthal, R.G., Faber, S.M., Flores, R., & Primack, J.R., *Astrophys. J.*, **301**, 27 (1986)
20. Law, David R., Steidel, Charles C., Erb, Dawn K., Larkin, James E., Pettini, M., Shapley, A. E., Wright, Shelley A., 2009. *submitted to Astrophys. J.*, 2009arXiv0901.2930L, 2009arXiv0901.2930L
21. Khochfar, S. & Burkert, A., *Astron. Astrophys.*, **445**, 403 (2006)
22. Dotti, M., Colpi, M., Haardt, F., & Mayer, L., Supermassive black hole binaries in gaseous and stellar circumnuclear discs: orbital dynamics and gas accretion, *Mon. Not. R. Astron. Soc.*, **379**, 956-962 (2007)
23. Kaufmann, T., Mayer, L., Wadsley, J., Stadel, J. & Moore, B., *Mon. Not. R. Astron. Soc.*, **370**, 1612 (2006)
24. Escala, A., Larson, R. B., Coppi, P. S., & Mardones, D., *Astrophys. J.*, **607**, 765 (2004)
25. Kitsionas, S. & Whitworth, S., *Mon. Not. R. Astron. Soc.*, **330**, 129 (2002)
26. Steinmetz, M. & White, S.D.M., *Mon. Not. R. Astron. Soc.*, **288**, 545 (1997)
27. Bate, M. & Burkert, A., *Mon. Not. R. Astron. Soc.*, **288**, 1060 (1997)



28. Nelson, A.F., *Mon. Not. R. Astron. Soc.*, **373**, 1039 (2006)
29. Dotti, M., Colpi, M. & Haardt, F., *Mon. Not. R. Astron. Soc.*, **367**, 103 (2006)
30. Spaans, M. & Silk, J., *Astrophys. J.*, **538**, 115 (2000)
31. Klessen, R.S., Spaans, M., Jappsen, A., *Mon. Not. R. Astron. Soc.*, **374**, L29 (2007)
32. Downes, D. & Solomon, P. M., *Astrophys. J.*, **507**, 615 (1998)
33. Wada, K., *Astrophys. J.*, **559**, L41 (2001)
34. Wada, K. & Norman, C., *Astrophys. J.*, **566**, L21 (2002)
35. Li, Y., Mac Low, M.M., & Klessen, R. S., Control of Star Formation in Galaxies by Gravitational Instability, *Astrophys. J.*, **650**, L19-L22 (2005)
36. Escala, A., Toward a Comprehensive Fueling-controlled Theory of the Growth of Massive Black Holes and Host Spheroids, *Astrophys. J.*, **671**, 1264 (2007)
37. Schaye, J. *Astrophys. J.*, 809, 667 (2004)
38. Omukai, K., Schneider, R., & Haiman, Z., Can Supermassive Black Holes Form in Metal-Enriched High Redshift Protogalaxies? *Astrophys. J.*, **686**, 801-814 (2008)
39. Begelman, M., Did Supermassive Black Holes Form by Direct Collapse?, *AIPC*, **990**, 489-493 (2008)
40. Pelupessy, F.I., di Matteo, T., & Ciardi, B., How Rapidly Do Supermassive Black Hole “Seeds” Grow at Early Times? *Astrophys. J.*, bf 665, 107 (2007)
41. Debattista, V. P., Mayer, L., Carollo, C. M., Moore, B., Wadsley, J., Quinn, T., The Secular Evolution of Disk Structural Parameters, *Astrophys. J.*, **645**, 209-227 (2006)
42. Mayer, L., Quinn, T., Wadsley, J. & Stadel, J., *Astrophys. J.*, **609**, 1045 (2004)
43. Durisen, R. H., Boss, A. P., Mayer, L., Nelson, A. F., Quinn, T., Rice, W. K. M, Gravitational Instabilities in Gaseous Protoplanetary Disks and Implications for Giant Planet Formation, Protostars and Planets V, B. Reipurth, D. Jewitt, and K. Keil (eds.), University of Arizona Press, Tucson, 951, 607-622 (2007)
44. Lodato, G. & Natarayan, P., Supermassive black hole formation during the assembly of pre-galactic discs, *Mon. Not. R. Astron. Soc.*, **371**, 1813 (2006)
45. Rice, W. K. M., Lodato, G. & Armitage, P. J., Investigating fragmentation conditions in self-gravitating accretion discs, *Mon. Not. R. Astron. Soc.*, **364**, L56-L60 (2005)
46. Nelson, A.F., Benz, W., Adams, F.C., & Arnett, D., Dynamics of Circumstellar Disks, *Astrophys. J.*, **502**, 342-371 (1998)
47. Shapiro, S.L., *Astrophys. J.*, Spin, Accretion, and the Cosmological Growth of Supermassive Black Holes **620**, 59-68 (2005)

48. Shapiro, S.L., & Teukolski, S.A., Black holes, white dwarfs and neutron stars. The Physics of Compact Objects, Wiley (1985)

49 . Djorgovski, S. G, Volonteri, M., Springel, V., Bromm, V. & Meylan, G. The Origins and the Early Evolution of Quasars and Supermassive Black Holes, Proc. XI Marcel Grossmann Meeting on General Relativity, eds. H. Kleinert, R.T. Jantzen & R. Ruffini, Singapore: World Scientific (Djorgovski, S. G, Volonteri, M., Springel, V., Bromm, V. & Meylan, G. The Origins and the Early Evolution of Quasars and Supermassive Black Holes, Proc. XI Marcel Grossmann Meeting on General Relativity, eds. H. Kleinert, R.T. Jantzen & R. Ruffini, Singapore: World Scientific (2008)

50. Soltan, A., Masses of quasars, *Mon. Not. R. Astron. Soc.*, **200**, 115-122 (1982)

51. Mo, H, Mao, S., & White, S.D.M. The formation of galactic discs, *Astrophys. J.*, **295**, 319-336 (1998)

52. Haiman, Z., *Astrophys. J.*, Constraints from Gravitational Recoil on the Growth of Supermassive Black Holes at High Redshift, **613**, 36 (2004)

53. Volonteri, M., & Rees, M.J., Quasars at  $z=6$ : The Survival of the Fittest, *Astrophys. J.*, **650**, 669 (2006)